Twenty-first century increases in total and extreme precipitation across the Northeastern USA

Christopher J. Picard[1] · Jonathan M. Winter[2] · Charlotte Cockburn[3] ·
Janel Hanrahan[4] · Natalie G. Teale[2] · Patrick J. Clemins[5] · Brian Beckage[5,6]

Abstract

The northeastern USA has experienced a dramatic increase in total and extreme precipitation over the past 30 years, yet how precipitation will evolve across the Northeast by the end of the twenty-first century remains uncertain. To examine the future of precipitation across the Northeast, we use the Weather Research and Forecasting (WRF) regional climate model driven by the National Center for Atmospheric Research Community Earth System Model (CESM) to simulate precipitation for historical (1976–2005) and future (2070–2099) periods. We compare precipitation from CESM-WRF hindcasts to gridded observations (Daymet), finding a 4.6% dry bias and 7.7% wet bias for total and extreme precipitation, respectively. CESM-WRF projections have increases in both total (9.7%) and extreme (51.6%) precipitation by the end of the twenty-first century, with winter having the largest increases in total precipitation (16.4%) and extreme precipitation (109.3%). These results are consistent with additional WRF simulations forced with the Max Planck Institute Earth System Model and the North American Coordinated Regional Downscaling Experiment archive. To investigate the drivers of precipitation change, we analyze several atmospheric variables and find that the projected increases in extreme precipitation are strongly related to increasing precipitable water over the eastern USA and the Atlantic Ocean. Understanding projected increases in total and extreme precipitation is critical for stakeholders to prepare for the impacts of intensified precipitation.

✉ Christopher J. Picard
    christopher.j.picard.23@dartmouth.edu

1   Dartmouth College, Hanover, NH, USA

2   Department of Geography, Dartmouth College, Hanover, NH, USA

3   Department of Earth Sciences, Dartmouth College, Hanover, NH, USA

4   Department of Atmospheric Sciences, Northern Vermont University-Lyndon, Lyndonville, VT, USA

5   Department of Computer Science, University of Vermont, Burlington, VT, USA

6   Department of Plant Biology, University of Vermont, Burlington, VT, USA

1 Introduction

The northeastern USA is both the most densely forested and populated region in the country, containing both large urban areas and remote rural communities (Dupigny-Giroux et al. 2018). The Northeast faces multiple hazards from climate change including altered total and extreme precipitation, which can cause flooding, damage infrastructure, reduce agricultural productivity, degrade ecosystems, and hurt tourism (Dupigny-Giroux et al. 2018). For example, enhanced total and extreme precipitation have the potential to destroy roads due to erosion and culvert failure (Rasmussen et al. 2018), increase weather-related crop losses (Wolfe et al. 2018), enhance agricultural runoff of pesticides and other chemicals (Bloomfield et al. 2006), harm vulnerable freshwater aquatic habitats (Jones et al. 2013), and ruin important cultural landmarks and recreational areas (New Hampshire Coastal Risk and Hazards Commission, 2016). Given these broad impacts, it is essential to understand historical and potential future changes in Northeast total and extreme precipitation.

1.1 Total precipitation

Over the past century, the northeastern USA has experienced increased annual precipitation (Hayhoe et al. 2007; Kunkel et al. 2013; Maloney et al. 2014; Walsh et al. 2014; Huang et al. 2017, 2020). Huang et al. (2017) found that total Northeast precipitation abruptly increased by 13% over 2002 to 2014; these results are consistent with Hayhoe et al. (2007) and Walsh et al. (2014). Hayhoe et al. (2007) determined that New England, New York, New Jersey, and Pennsylvania experienced an increase of 10 mm decade^{-1} in annual total precipitation over the twentieth century, while Walsh et al. (2014) reported an 8% increase in Northeast precipitation since 1991, relative to 1901–1960.

The observed increases in total annual precipitation across the northeastern USA are expected to intensify during the twenty-first century due to climate change. Guilbert et al. (2014) found that mean daily precipitation over the Lake Champlain Basin in Vermont is projected to increase by 7.1% and 9.9% by the middle and late twenty-first century, respectively. These findings agree with Hayhoe et al. (2007) who calculated annual total precipitation increases of 7 to 14%, depending on the emissions scenario, by the end of the century across the northeastern USA. Maloney et al. (2014) analyzed an ensemble of Coupled Model Intercomparison Project Phase 5 (CMIP5) simulations and found that Northeast total precipitation is projected to increase by 5–10% in the near-future (2009–2038) and 15–25% by the late twenty-first century (2069–2098).

While total annual precipitation is expected to increase, simulated precipitation changes are not evenly distributed across the year. Previous studies suggest that climate change will significantly increase winter precipitation (Hayhoe et al. 2007; Lynch et al. 2016) and either have no effect on or decrease summer precipitation by the late twenty-first century (Hayhoe et al. 2007). An evaluation of CMIP5 model projections by Lynch et al. (2016) over New England and parts of Canada indicates significant increases in precipitation across spring, fall, and winter, with the most robust late century (2071–2100) increases occurring in the winter (20.9 mm month^{-1}) and spring (20.6 mm month^{-1}). However, the 16 global climate models (GCMs) used by Lynch et al. (2016) did not agree on the direction of future precipitation change during July, August, and September, with evidence of weak drying during the late summer and

early fall despite an annual increase in precipitation. Consistent with these findings, Hayhoe et al. (2007) used nine GCM simulations to conclude that total precipitation will experience about a 30% increase during the winter by 2070–2099, whereas summer total precipitation will remain virtually unchanged.

1.2 Extreme precipitation

The Northeast has experienced the largest increase in 99th percentile wet day precipitation (hereafter extreme precipitation) in the nation (Kunkel et al. 2013). Easterling et al. (2017) found that the Northeast experienced an approximate 55% increase in extreme precipitation between 1958 and 2016. Hoerling et al. (2016) also calculated an increase in observed heavy precipitation (95th percentile wet day precipitation) across the Northeast of about 30% over 1979–2013, consistent with the broader trend over 1901–2013. Frei et al. (2015) found that extreme precipitation in 2001–2012 was significantly larger than during previous periods (e.g., 1977–1988), but also highlighted that precipitation trends are highly sensitive to start and end date. Consistent with Frei et al. (2015), Huang et al. (2017) discovered a change point in 1996 where extreme precipitation increased by 53% over 1996–2014 compared to the historical 1901–1995 mean. Huang et al. (2018) revealed that tropical cyclones were responsible for almost half (48%) of the post-1996 extreme precipitation increase, with fronts and extratropical cyclones contributing 25% and 15%, respectively. Huang et al. (2021) attributed the post-1996 increase in Northeast extreme precipitation to internal Atlantic sea surface temperature variability, anthropogenic aerosols, and greenhouse gasses.

Recent studies indicate that the Northeast is projected to experience significant increases in extreme precipitation over the twenty-first century. Maloney et al. (2014) focused on projecting extreme precipitation in the Northeast, finding that the number of heavy rainfall events (precipitation > 25 mm day^{-1}) are projected to increase four to five times by 2069–2098. Hayhoe et al. (2018) projected increases in Northeast extreme precipitation of over 40% by the late twenty-first century relative to 1986–2015. Thibeault and Seth (2014) found increases of 57.6% and 100.4% in extreme precipitation by the middle (2041–2070) and late (2071–2099) twenty-first century compared to historical (1961–1990) values, respectively. Akinsanola et al. (2020) used 12 Coupled Model Intercomparison Project Phase 6 (CMIP6) climate model simulations to explore summer and winter changes in extreme precipitation events and found that precipitation is projected to increase during both seasons by the late twenty-first century, with larger increases during the winter. Thibeault and Seth (2014) also found larger increases in winter wet extremes relative to summer wet extremes, with winter extreme precipitation changes strongly influencing the projected increases in total annual precipitation.

1.3 Objectives

This study adds to the existing literature by analyzing multiple simulations from a regional climate model explicitly calibrated and evaluated over the Northeast as well as comparing those model runs to an additional 16 simulations from the North American Coordinated Regional Downscaling Experiment archive. Previous RCM studies of Northeast precipitation, such as Loikith et al. (2018) and Huang et al. (2020), focus on model evaluation and do not include simulations of future climate. Thus, there remains a need to examine high-resolution regional climate model simulations of future total and extreme precipitation over the Northeast USA, as well as compare the atmospheric drivers of precipitation changes

from regional climate model simulations to those found using GCMs. This study adds to the existing literature by analyzing multiple simulations from a regional climate model explicitly calibrated and evaluated over the Northeast as well as comparing those model runs to an additional 16 simulations from the NA-CORDEX archive. Leveraging this broad ensemble, we quantify changes in multiple aspects of extreme precipitation, including intensity, frequency, distribution, seasonality, and spatial patterns. In addition, we identify the large-scale atmospheric patterns associated with extreme precipitation across the Northeast and examine changes in those patterns to assess possible drivers of extreme precipitation change. Our findings have implications for flood preparedness and infrastructure planning, while also providing insights into the necessary adaptations to preserve the environment and economy of the Northeast.

2 Data and methods

2.1 Regional climate model simulations and observed data

We used the National Center for Atmospheric Research Weather Research and Forecasting model v3.9.1 (Skamarock et al. 2008) to generate high-resolution climate simulations. RCMs resolve processes that are not captured bycoarser resolution global climate models and can be tailored for specificclimate dynamics and impacts (Gutowski et al. 2020). However, the accuracy of RCMs is heavily influenced by errors in the GCM boundary conditions, choice of parameterization schemes, and complexity of the landscape (e.g., mountains, coasts). Loikith et al. (2018), using the NASA-Unified WRF model, found a wet bias for mean precipitation and a cold bias for mean temperature during the cool season in the Northeast. Similarly, Huang et al. (2020) used five WRF simulations with unique physics configurations over the Lake Champlain basin and found consistent wet and cold biases.

Our WRF configuration was based on Huang et al. (2020), who compared five uniquely parameterized WRF simulations over the Lake Champlain basin. Huang et al. (2020) found that all simulations had similar skill in modeling mean temperature and precipitation, but simulations of extreme temperature and precipitation were generally less accurate and more variable across model configurations. Out of the five configurations, Huang et al. (2020) determined that the RNWM — rapid radiative transfer model for GCMs (RRTMG) radiation scheme (Iacono et al. 2008), the new simplified Arakawa-Schubert (New SAS) cumulus scheme (Han & Pan 2011), the WRF Single-Moment 6-Class microphysics scheme (Hong & Lim 2006), and the MYJ planetary boundary layer scheme (Mesinger 1993; Janjić 1994) — was the optimal configuration for simulating total and extreme precipitation over the Lake Champlain Basin. The selection of the New SAS cumulus scheme by Huang et al. (2020) is consistent with Bruyère et al. (2017), who found that the Kain-Fritsch cumulus scheme overestimated precipitation compared to New SAS.

We used a model domain of 69×69 grid points (latitude × longitude) with a 36 km resolution set over the eastern USA (Fig. 1). For our analysis, we trimmed the domain to include only the Northeast states (Fig. 1), which we define as New Hampshire, Vermont, Massachusetts, Connecticut, Rhode Island, Maine, New York, Pennsylvania, New Jersey, Delaware, Maryland, Washington, D.C., and West Virginia, consistent with Walsh et al. (2014) and Huang et al. (2017, 2018, 2021). We chose a 36 km resolution for WRF simulations to prioritize spatial coverage and computational efficiency. While ideally simulations would have been run at a higher resolution as well, both Loikith et al. (2018) and Huang
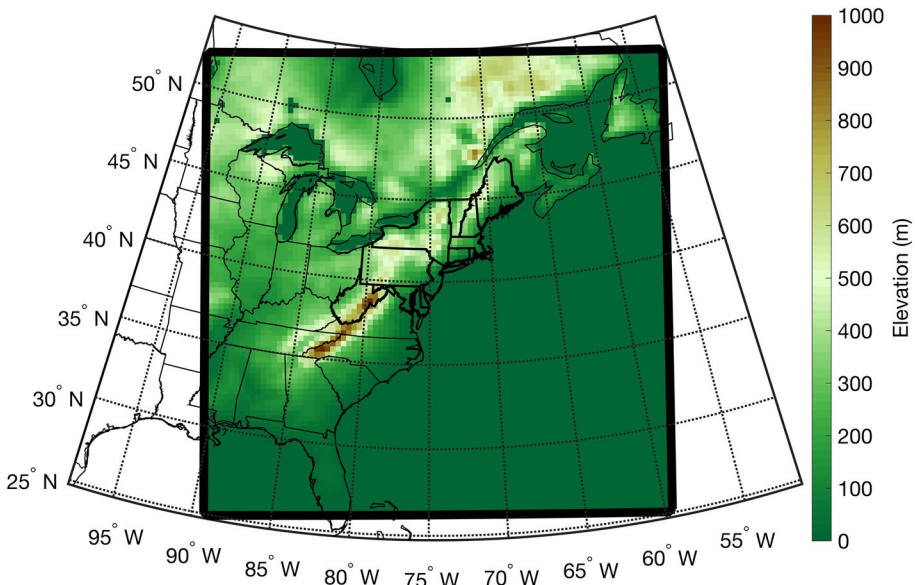
Fig. 1 WRF domain and elevation with Northeast states bolded

et al. (2020) found that coarser spatial resolution does not degrade the quality of modeled precipitation. Loikith et al. (2018) compared NASA-unified WRF model simulations of the Northeast at 24, 12, and 4 km horizontal resolutions, and showed that higher resolution simulations of precipitation are not more accurate than lower resolution simulations of precipitation. Similarly, Huang et al. (2020) showed that between 36, 12, and 4 km resolution WRF simulations, the 36 km simulations have the smallest annual precipitation biases compared to Daymet over the Lake Champlain Basin.

We compared historical simulations of WRF forced with bias-corrected National Center for Atmospheric Research Community Earth System Model data (CESM-WRF) to Daymet, a daily gridded observational dataset from the Oak Ridge National Laboratory Distributed Active Archive Center (Thornton et al. 1997, 2016). Daymet data are available for North America at a 1-km spatial resolution from 1980 to the present. We directly compared Daymet data with CESM-WRF simulations by first upscaling Daymet to match the spatial resolution of our CESM-WRF simulations (36 km resolution) and then using linear interpolation to map Daymet to the WRF grid. Daymet is a land-based observational product; therefore, we removed grid cells dominated by water (e.g., Lake Ontario and Atlantic Ocean) from our CESM-WRF simulations using the Daymet landmask. All Daymet analyses in this study were conducted over the period of 1980–2005.

To contextualize our CESM-WRF results, we ran additional WRF simulations using boundary conditions from the Max Planck Institute Earth System Model (ESM-WRF). The configuration of WRF in CESM-WRF and ESM-WRF was identical. We further evaluated our CESM-WRF results using 16 simulations (Table S1) from the North American Coordinated Regional Downscaling Experiment (NA-CORDEX; Mearns et al. 2017). NA-CORDEX RCM simulations cover the majority of North America at high spatial resolution and are forced by GCM outputs from CMIP5. Non-bias corrected NA-CORDEX outputs were used in this study because we only assessed changes between future and historical

simulations (reducing the impacts of biases) and at the time of analysis there were errors in the bias-corrected NA-CORDEX data (McGinnis 2021). Further, we calculated NA-COR-DEX precipitation changes by amount (mm/year) in addition to percentage, as percentage uses historical precipitation and therefore could be sensitive to using non-bias corrected simulations, and found similar results (not shown).

Our historical and future CESM-WRF simulations spanned 1976–2005 and 2070–2099, respectively. Both historical and future simulations were run in 5-year time slices with a 6-month spin-up. For example, the simulation for 1976–1980 was initialized July 1st of 1975, and then the simulation for 1981–1985 was initialized on July 1st of 1980. WRF, CESM, and ESM boundary conditions along with NA-CORDEX simulations were run under Representative Concentration Pathway (RCP) 8.5 (Moss et al. 2010). We also ran our WRF simulations under RCP 4.5 to examine the sensitivity of our results to greenhouse gas emissions scenario.

2.2 Precipitation indices

There are a variety of definitions for extreme precipitation, which typically incorporate attributes such as threshold or metric, timescale, and spatial scale (Barlow et al. 2019). We define extreme precipitation (EP) as the amount of precipitation falling during the top 1% of wet days (99th percentile wet days; Walsh et al. 2014; Frei et al. 2015; Easterling et al. 2017; Huang et al. 2017, 2018, 2020). While this definition is used extensively and allows us to compare our results to previous studies, we caveat that 99th percentile wet days do not necessarily cause societal impacts. Extreme precipitation thresholds were determined for each grid cell by finding the 1% of wet days (precipitation > 1 mm day^{-1}) with the most precipitation across all 30 years (26 years for Daymet analyses) in a given grid cell. When comparing historical and future EP, we used the historical thresholds for both time periods to show how EP is projected to change over the century relative to historical EP. We calculate separate EP thresholds for CESM-WRF, Daymet, ESM-WRF, and each NA-CORDEX simulation annually and by season, consistent with previous literature (e.g., Huang et al. 2017). We define spring as March, April, and May (MAM), summer as June, July, and August (JJA), fall as September, October, and November (SON), and winter as December, January, and February (DJF). We define total precipitation (TP) as the annual (or seasonal) sum of precipitation on wet days. Definitions of EP and TP match indices described by the Expert Team on Climate Change Detection and Indices (ETCCDI; Zhang et al. 2011). The 1 mm day^{-1} threshold for wet days is chosen for consistency with previous studies including ETCCDI, as well as the fact that rain gauges, from which Daymet data are derived, can struggle to accurately capture rainfall measurements under 1 mm (Zhang et al. 2001). The frequencies of TP and EP are calculated by taking the average number of wet days and EP days over the Northeast, and the intensity is the average amount of TP that falls on wet days and EP that falls on EP days. We evaluated the statistical significance of changes in precipitation using the two sample Kolmogorov–Smirnov test (K-S test), a nonparametric goodness-of-fit test, using a significance level of $p < 0.05$.

2.3 Analysis of atmospheric dynamics

We assessed potential atmospheric drivers of EP changes by comparing historical (1986–1995) and future (2081–2090) precipitable water, 500 mb winds, and sea level

pressure. For each potential atmospheric driver, we first created EP day anomaly maps by subtracting the composite of that driver on all days from the composite of that driver on EP days. Identifying the patterns of potential atmospheric drivers associated with EP in both historical and future periods provides a general impression of the atmospheric drivers associated with EP days and whether these patterns change in the future.

To examine temporal changes in atmospheric dynamics we then calculated the differences (future minus historical) for each potential atmospheric driver on EP days, where consistencies between these differences and the anomaly pattern suggest a shift toward more favorable conditions for EP days in the future.

Finally, we quantified how close the potential atmospheric driver anomaly patterns are on each historical and future EP day relative to the average historical EP day. We first calculated the potential atmospheric driver anomaly pattern for each historical and future EP day. We then averaged the anomaly patterns for all historical EP days and subtracted that composite from the potential atmospheric driver anomaly patterns for each historical and future EP day. Finally, we took the root mean squared deviation (RMSD) of this difference, and then plotted the result against the magnitude of the EP event. By quantifying the difference between potential atmospheric driver anomaly patterns for each EP day and the historical average EP day, we can better understand how historical and future anomalies for each potential atmospheric driver connect to EP events and the projected changes in frequency and intensity of EP. We provide an example of this analysis in Fig. S1.

The domain for the atmospheric dynamics analyses is shown in Fig. 1 and similar to the precipitation analysis domain, but with water bodies, states outside of the Northeast, and Canada. We examined potential atmospheric drivers over two 10-year periods that fall in the middle of the historical (1976–2005) and future (2070–2099) periods used for our precipitation analysis to ensure feasibility both in terms of computational processing and data storage (atmospheric drivers require writing out three dimensional fields).

3 Results

We first compare annual and seasonal historical CESM-WRF total and extreme precipitation with Daymet to assess the accuracy of our model simulations. Second, we analyze the annual and seasonal differences between future and historical total and extreme precipitation using CESM-WRF. Third, we compare projections of total and extreme precipitation across CESM-WRF, ESM-WRF, and the NA-CORDEX archive. Finally, we contrast future and historical atmospheric dynamics to identify the drivers of the projected changes in extreme precipitation.

3.1 Total precipitation biases

Spatially averaged, CESM-WRF simulations of annual total precipitation (TP; sum of precipitation across wet days) have a small (54.6 mm; 4.6%) dry bias compared to Daymet between 1980 and 2005 (Table 1), with maximum biases generally less than 300 mm (Fig. 2). We find that CESM-WRF underestimates TP in the southern New England states, including Massachusetts, Rhode Island, and Connecticut. TP is simulated best in the southern and western parts of the Northeast, such as central Pennsylvania and western New York, with some wet biases in central New York, southwestern Pennsylvania, and West Virginia (Fig. 2). CESM-WRF simulates an excess of wet days, annually and throughout

Table 1 Biases in total wet day precipitation (TP), the number of wet days, and TP intensity between CESM-WRF and Daymet (1980–2005). Numbers in the table reflect the regional average. Statistically significant ($p < 0.05$) biases have an asterisk

	CESM-WRF	Daymet	Bias
Annual:			
Total precipitation	1,127.4 mm/year	1,182.0 mm/year	-4.6%
Wet days	149.6 days/year	123.9 days/year	+20.7%*
Intensity	5.3 mm	6.9 mm	-23.2%*
Spring:			
Total precipitation	305.6 mm/year	304.5 mm/year	+0.4%
Wet days	39.3 days/year	33.4 days/year	+17.7%*
Intensity	5.5 mm	6.6 mm	-16.7%*
Summer:			
Total precipitation	318.5 mm/year	307.4 mm/year	+3.6%
Wet days	47.1 days/year	31.0 days/year	+51.9%*
Intensity	5.7 mm	8.3 mm	-31.3%*
Fall:			
Total precipitation	235.9 mm/year	311.4 mm/year	-24.3%*
Wet days	30.5 days/year	29.6 days/year	+3.0%
Intensity	5.1 mm	7.2 mm	-29.2%*
Winter:			
Total precipitation	248.9 mm/year	240.8 mm/year	+3.4%
Wet days	32.7 days/year	29.9 days/year	+9.4%*
Intensity	4.6 mm	5.5 mm	-16.4%*

each season, compared to Daymet observations (Table 1). The excess number of wet days is offset by CESM-WRF's tendency to simulate lower precipitation intensity (less rainfall per wet day) than Daymet. Specifically, CESM-WRF simulated mean wet day precipitation is 23.2% less than Daymet, but CESM-WRF simulates 20.7% more wet days per year than Daymet, leaving an annual TP bias of -4.6% (Table 1).
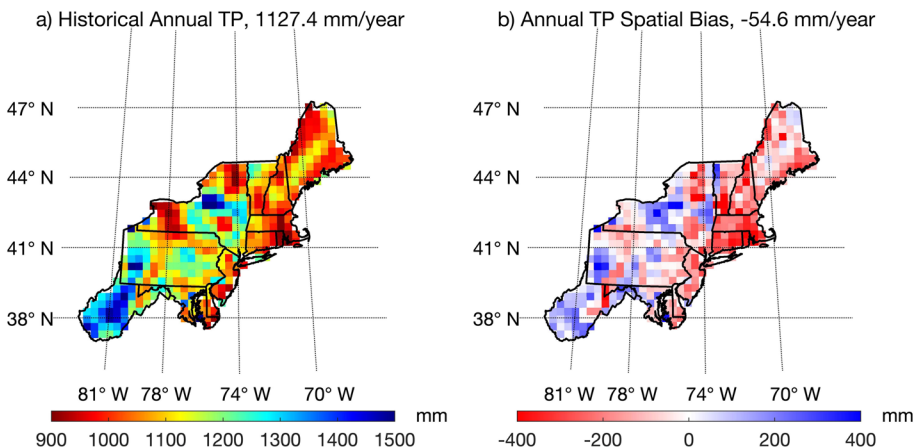

Fig. 2 Spatial distribution of **a** CESM-WRF historical (1980–2005) total precipitation and **b** total precipitation bias between CESM-WRF historical and Daymet (1980–2005)

The seasonal breakdown of TP also contains small biases for spring, summer, and winter; however, during the fall, CESM-WRF simulates a statistically significant 24.3% dry bias (Table 1). This large fall dry bias in CESM-WRF is a result of a small positive bias in the frequency of wet days coupled with a larger negative bias in intensity. Spatial patterns of CESM-WRF TP spring, summer, and winter biases are similar to the spatial pattern of the CESM-WRF TP annual bias; however, in the fall, TP is almost uniformly underestimated across the Northeast (Fig. S2).

ESM-WRF simulations also overestimate TP in spring, summer, and winter, and underestimate TP in fall (Table S2). Like CESM-WRF, ESM-WRF overestimates wet day frequency but underestimates wet day intensity annually and for all seasons (Table S2).

3.2 Extreme precipitation biases

Biases in extreme precipitation (EP; sum of precipitation on top 1% of wet days) are larger than TP biases, however the differences between CESM-WRF and Daymet EP are statistically insignificant annually and across all seasons (Table 2). CESM-WRF simulations have an EP wet bias of 7.7% annually (Fig. 3) and between 21 and 30% for all seasons except the fall, where EP is underestimated by 22.6% (Table 2). Across the Northeast, yearly EP biases have a west to east gradient with West Virginia, western Pennsylvania, and central New York having notable wet biases, states along the Atlantic coast having dry biases, and the center of the region being simulated most accurately (Fig. 3).

Although overall EP biases are insignificant, biases in EP frequency are significant annually and in summer and fall, and biases in EP intensity are significant annually and for all seasons (Table 2). CESM-WRF EP and TP frequency biases are similar in magnitude, with CESM-WRF simulating 22.3% more EP days than Daymet. CESM-WRF simulates

Table 2 Biases in total extreme precipitation (EP), the number of EP days, and EP intensity between CESM-WRF and Daymet (1980–2005). Numbers in the table reflect the regional average. Statistically significant ($p < 0.05$) biases have an asterisk

	CESM-WRF	Daymet	Bias
Annual:			
Extreme precipitation	71.3 mm/year	66.2 mm/year	+7.7%
EP days	1.48 days/year	1.21 days/year	+22.3%*
Intensity	44.0 mm	48.1 mm	-8.5%*
Spring:			
Extreme precipitation	17.6 mm/year	14.5 mm/year	+21.4%
EP days	0.37 days/year	0.31 days/year	+19.4%
Intensity	42.3 mm	42.4 mm	-0.2%*
Summer:			
Extreme precipitation	19.7 mm/year	15.2 mm/year	+29.6%
EP days	0.45 days/year	0.29 days/year	+55.2%*
Intensity	40.2 mm	50.9 mm	-21.0%*
Fall:			
Extreme precipitation	14.4 mm/year	18.6 mm/year	-22.6%
EP days	0.29 days/year	0.28 days/year	+3.6%*
Intensity	46.1 mm	56.1 mm	-17.8%*
Winter:			
Extreme precipitation	14.8 mm/year	11.7 mm/year	+26.5%
EP days	0.31 days/year	0.27 days/year	+14.8%
Intensity	42.1 mm	38.8 mm	+8.5%*

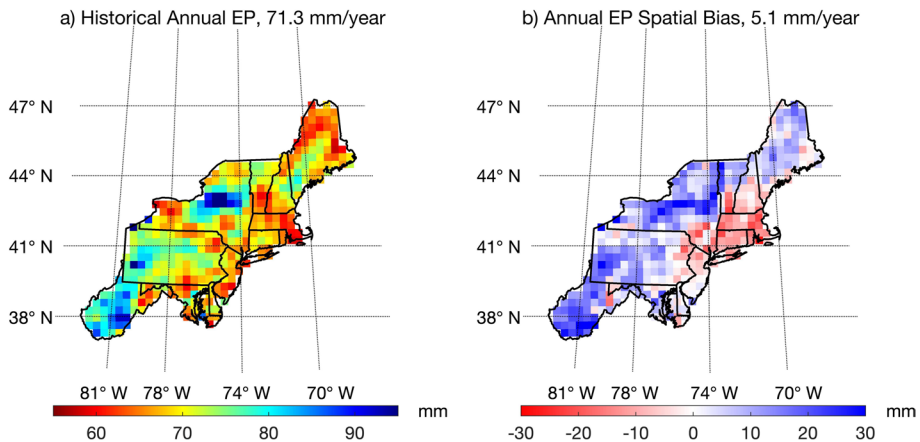**Fig. 3** Spatial distribution of **a** CESM-WRF historical (1980–2005) extreme precipitation and **b** extreme precipitation bias between CESM-WRF historical and Daymet (1980–2005)

higher EP event frequency but lower EP event intensity than Daymet. As with TP, these two compensating biases result in an insignificant yearly total EP bias of approximately 7.7% (Table 2).

The spring and summer spatial patterns of EP bias are consistent with the annual spatial pattern of EP bias (Fig. S3). However, the winter wet bias is present across most of the domain, and the fall dry bias is relatively uniform across the domain with only a few areas showing wet biases, including West Virginia and the area surrounding Albany, NY (Fig. S3). Biases in frequency partially offset biases in intensity during the summer, but not during the other seasons, and fall is the only season with a dry bias in EP, a result of WRF simulating slightly more frequent but substantially less intense EP days than Daymet (Table 2).

ESM-WRF simulates more EP than CESM-WRF, with an annual EP bias of 26.6% (Table S3). ESM-WRF overestimates EP in every season, with significant biases in summer and winter (Table S3). Excess ESM-WRF EP is the result of too many EP days combined with greater EP intensity relative to Daymet, except in summer where EP intensity is underestimated.

3.3 Changes in total precipitation

Northeast annual total precipitation is projected (CESM-WRF under RCP 8.5) to increase 9.7% by the end of the twenty-first century (2070–2099) relative to the historical period (1976–2005; Table 3, Fig. 4), consistent with ESM-WRF simulations (Table S4). Virtually all the Northeast is expected to have increases in annual TP, but the largest changes are projected to occur in West Virginia, central New York, the Lake Champlain Basin, and northern Maine (Fig. 4b). Annually, CESM-WRF simulations reveal almost no change in the average number of wet days, but a statistically significant 7.6% increase in TP intensity (Table 3). Similarly, ESM-WRF simulations have a significant increase in wet day intensity and a smaller (though significant) decrease in the number of wet days (Table S4). These findings indicate that intensity, instead of frequency, drives simulated increases in annual precipitation (Table 3).

Table 3 Difference between future (2070–2099) and historical (1976–2005) total wet day precipitation (TP), the number of wet days, and TP intensity for CESM-WRF. Numbers in the table reflect the regional average. Statistically significant ($p < 0.05$) changes have an asterisk

	Historical	Future	Change
Annual:			
Total precipitation	1128.0 mm/year	1237.4 mm/year	+9.7%*
Wet days	149.2 days/year	149.5 days/year	+0.2%
Intensity	5.3 mm	5.7 mm	+7.6%*
Spring:			
Total precipitation	308.0 mm/year	342.3 mm/year	+11.1%*
Wet days	39.5 days/year	40.2 days/year	+1.8%
Intensity	5.5 mm	6.0 mm	+9.1%*
Summer:			
Total precipitation	332.3 mm/year	378.0 mm/year	+13.8%*
Wet days	46.7 days/year	47.7 days/year	+2.1%
Intensity	5.7 mm	6.3 mm	+10.5%*
Fall:			
Total precipitation	236.5 mm/year	224.6 mm/year	-5.0%
Wet days	30.2 days/year	27.7 days/year	-8.3%*
Intensity	5.1 mm	5.2 mm	+2.0%
Winter:			
Total precipitation	251.2 mm/year	292.5 mm/year	+16.4%*
Wet days	32.8 days/year	33.9 days/year	+3.4%
Intensity	4.6 mm	5.3 mm	+15.2%*

Spring, summer, and winter are projected to have statistically significant increases in TP by the end of the century, with winter having the largest increase of 16.4% (Table 3, Fig. S4). The simulated increases in winter and spring precipitation from CESM-WRF agree with ESM-WRF; however, the two models disagree on the direction and magnitude of change during the summer and fall seasons (Table 3, S4). Although CESM-WRF and ESM-WRF disagree on total precipitation changes during the fall, both simulate fewer wet days and more intense fall TP by the end of the twenty-first century (Table 3, S4). In contrast, spring, summer, and winter wet days each year are virtually unchanged in both
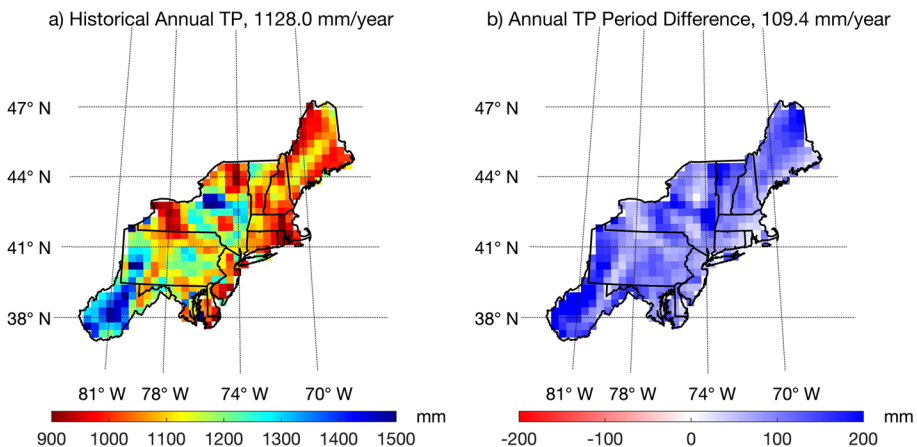

Fig. 4 Average **a** CESM-WRF historical (1976–2005) total precipitation and **b** difference between CESM-WRF future (2070–2099) and historical total precipitation across the Northeast

CESM-WRF and ESM-WRF projections (Table 3, S4). Here, the projected changes in TP across these three seasons are primarily due to increases in the amount of precipitation on wet days, with the largest changes occurring during the winter (Table 3, S4). CESM-WRF projections of TP under RCP 8.5 are qualitatively consistent with CESM-WRF projections under RCP 4.5, though changes are smaller in magnitude and generally insignificant due to the lower radiative forcing (Table S6).

Outputs from the 16 GCM-RCM pairs in the NA-CORDEX archive are consistent with CESM-WRF and ESM-WRF results, with 13 of 16 simulations projecting statistically significant increases in annual TP (Table S8–S23). NA-CORDEX simulations generally agree with CESM-WRF and ESM-WRF for winter and spring, with 14 out of 16 NA-CORDEX simulations projecting statistically significant increases in winter TP and 12 out of 16 NA-CORDEX simulations projecting significant increases in spring TP (Table S8–S23). NA-CORDEX simulations provide further evidence that the projected annual TP increases are driven by winter and spring TP increases. NA-CORDEX simulations agree with the lack of a significant change in TP during the fall projected by both CESM-WRF and ESM-WRF. However, during the summer only 3 NA-CORDEX simulations project significant TP increases, which is consistent with ESM-WRF but not CESM-WRF (Table S8–S23). A summary of the magnitude of annual and seasonal TP projections for the NA-CORDEX models, with CESM-WRF and ESM-WRF plotted for reference, is shown in Fig. 5.

3.4 Changes in extreme precipitation

Over the twenty-first century EP is projected (CESM-WRF under RCP 8.5) to increase an average of 51.6% across the Northeast (Table 4, Fig. 6b). As with TP, almost the entire domain experiences increased EP with West Virginia, parts of Pennsylvania, central New
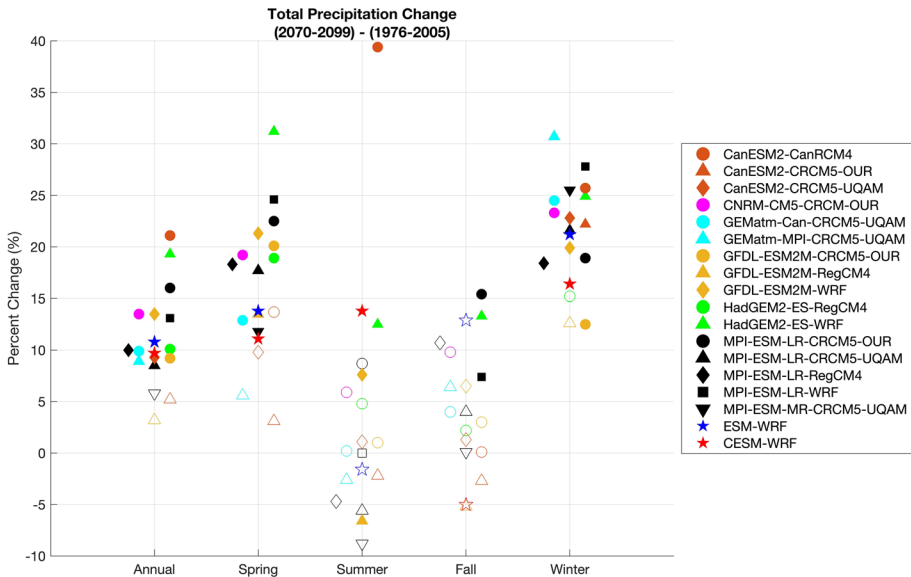

Fig. 5 Projected changes in annual and seasonal total precipitation for all NA-CORDEX simulations, ESM-WRF, and CESM-WRF. Statistically significant ($p < 0.05$) changes have filled in markers

Table 4 Difference between future (2070–2099) and historical (1976–2005) extreme precipitation (EP), the number of EP days, and EP intensity for CESM-WRF. Numbers in the table reflect the regional average. Statistically significant ($p < 0.05$) have an asterisk

	Historical	Future	Change
Annual:			
Extreme precipitation	72.3 mm/year	109.6 mm/year	+51.6%*
EP days	1.48 days/year	2.20 days/year	+48.7%*
Intensity	44.4 mm	44.8 mm	+0.9%
Spring:			
Extreme precipitation	17.8 mm/year	33.6 mm/year	+88.8%*
EP days	0.38 days/year	0.69 days/year	+81.6%*
Intensity	42.5 mm	43.2 mm	+1.7%
Summer:			
Extreme precipitation	20.6 mm/year	29.5 mm/year	+43.2%*
EP days	0.45 days/year	0.65 days/year	+44.4%*
Intensity	40.0 mm	39.4 mm	-1.5%
Fall:			
Extreme precipitation	15.3 mm/year	17.4 mm/year	+13.7%
EP days	0.28 days/year	0.34 days/year	+21.4%
Intensity	47.4 mm	47.8 mm	+0.8%
Winter:			
Extreme precipitation	15.0 mm/year	31.4 mm/year	+109.3%*
EP days	0.31 days/year	0.64 days/year	+106.5%*
Intensity	42.5 mm	43.2 mm	+1.7%

York, the Lake Champlain Basin, and northeastern Maine recording the largest increases (Fig. 6). Compared to CESM-WRF, the ESM-WRF EP increase (104.2%) is substantially higher (Table S5). Despite the widespread increases of EP inland, slight reductions in EP are projected for several grid cells along the Atlantic coast with fall coastal drying most heavily influencing this spatial pattern (Fig. 6, S5). CESM-WRF simulations reveal a 48.7%
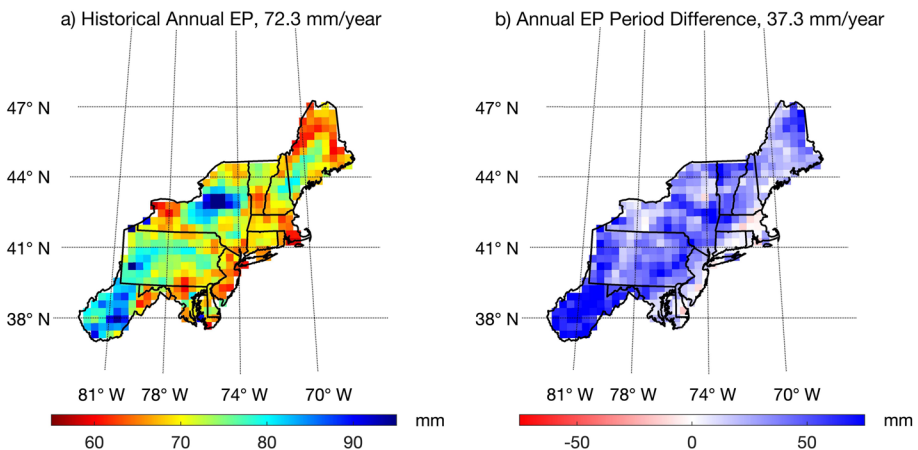

Fig. 6 Average **a** CESM-WRF historical (1976–2005) extreme precipitation and **b** difference between CESM-WRF future (2070–2099) and historical extreme precipitation across the Northeast

increase in the number of EP days per year, but almost no change in EP intensity (Table 4). Similarly, ESM-WRF projects a 94.1% increase in frequency and only a minor intensity increase, therefore emphasizing that frequency rather than intensity drives simulated future EP increases (Table S5). Figure 7a and b show the historical and future distributions of annual and daily EP, respectively, for CESM-WRF. There are no years in 2070–2099 with EP less than 50 mm, and eight unprecedented years of annual EP exceeding 125 mm. Figure 7b clearly displays the marked increase in the frequency of all EP days, and also highlights the increase in the frequency of the most extreme EP days (> 100 mm), with several unprecedented events (> 175 mm; not shown).

CESM-WRF simulations indicate that each season is projected to experience a domain average increase in EP, but the magnitudes of these changes vary. Winter EP is projected to increase by 109.3%, whereas the fall increase is insignificant (Table 4). ESM-WRF simulates a significant winter and fall increase in EP (Table S5). Both CESM-WRF and ESM-WRF have statistically significant increases in spring EP (88.8% and 137.9%, respectively), suggesting that spring may also be an important driver of future EP change (Table 4, S5). With the exception of the fall, all seasons are projected to experience significant increases in EP frequency, with winter and spring having the most marked changes of 106.5% and 81.6%, respectively (Table 4). Conversely, seasonal changes in EP intensity for CESM-WRF are insignificant and range from -2% and 2%, in agreement with ESM-WRF for all seasons except the fall (Table S5). Although spatial changes in EP vary across seasons, CESM-WRF projects that EP consistently increases in West Virginia, parts of Pennsylvania, and northeastern Maine (Fig. S5), similar to ESM-WRF (not shown). Areas of decreasing EP include the New England coast in fall and winter, and western New York in summer (Fig. S5).

NA-CORDEX simulations contain statistically significant increases annually and during the spring and winter for all GCM-RCM pairs. The increases in annual EP range from 47.9% (Table S39) to 169.3% (Table S24) which suggests that the CESM-WRF projections are conservative. The largest seasonal percentage EP change in the NA-CORDEX simulations (Table S24–S39) occurs either in the winter (10 simulations) or the spring (6 simulations). This finding strengthens the evidence that wintertime EP events are expected
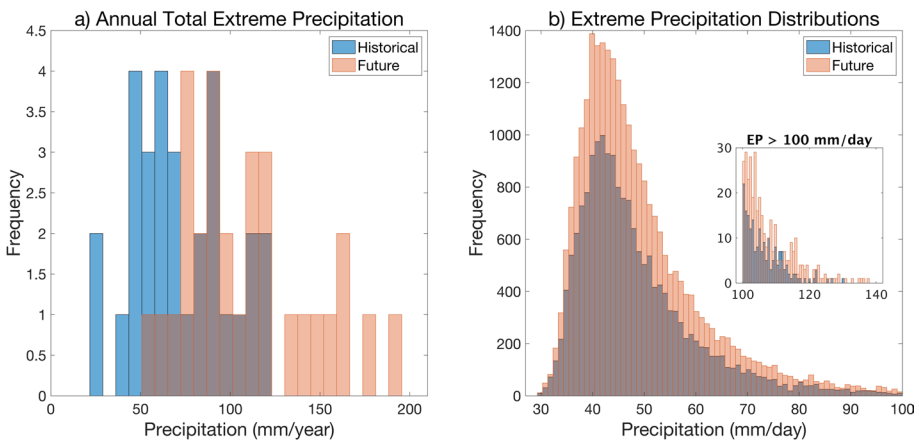

Fig. 7 Histograms of **a** CESM-WRF spatially averaged annual extreme precipitation for historical (1976–2005) and future (2070–2099) periods and **b** CESM-WRF daily extreme precipitation for each grid cell over all 30 years of the historical and future periods

to play an important role in annual TP and EP increases across the Northeast, consistent with CESM-WRF and ESM-WRF simulations. Most NA-CORDEX simulations also have significant increases in summer and fall EP, but percentage changes are smaller in magnitude than during the colder months. Annual and seasonal EP differences between the 2070–2099 and 1976–2005 for the NA-CORDEX models, CESM-WRF, and ESM-WRF are shown in Fig. 8. Across ESM-WRF, CESM-WRF, and the ensemble of NA-CORDEX simulations, Fig. 8 highlights the importance of winter and spring EP increases to the annual change over the Northeast.

3.5 Atmospheric drivers of projected precipitation changes

We analyzed the drivers of future extreme precipitation change in the Northeast using a suite of atmospheric variables from the CESM-WRF model runs. Figure 9a and b show the precipitable water anomaly (average precipitable water on EP days minus average precipitable water on all days) in the historical and future periods, respectively. Both historical and future anomalies show marked increases in precipitable water over the eastern USA on EP days compared to all days (Fig. 9a, b), confirming the expectation that EP is associated with increased moisture. Consistent with the large increases in EP described above, we find that the average EP day in the future has 6.25 mm (23.8%) more precipitable water than the average EP day in the historical record (Fig. 9c). The largest future increases in precipitable water are projected to be over the Atlantic Ocean and across the southern continental USA. Precipitable water increases at higher latitudes are still projected to be substantial,
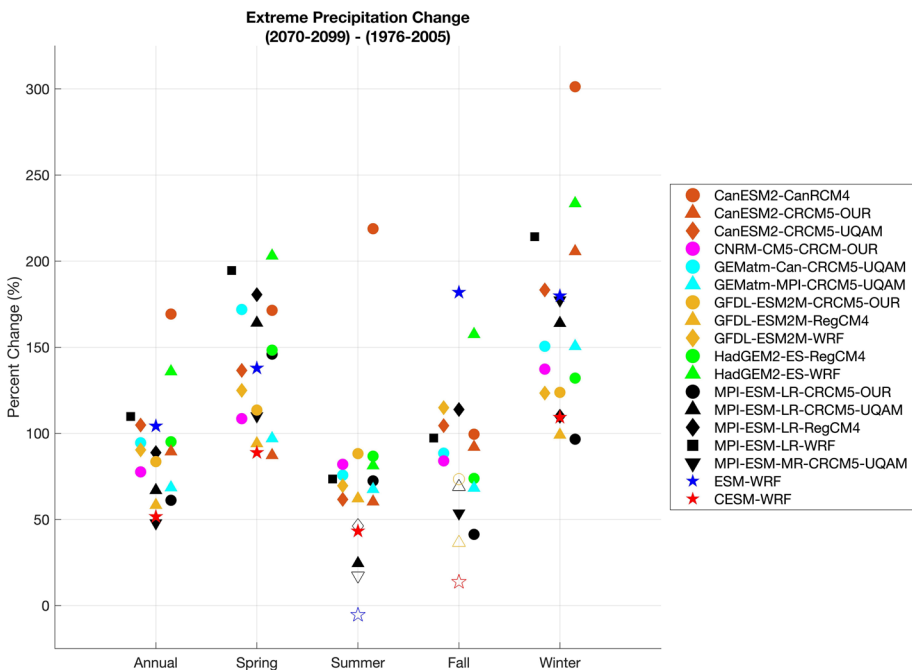

Fig. 8 Projected changes in annual and seasonal total extreme precipitation for all NA-CORDEX simulations, ESM-WRF, and CESM-WRF. Statistically significant ($p < 0.05$) changes have filled in markers
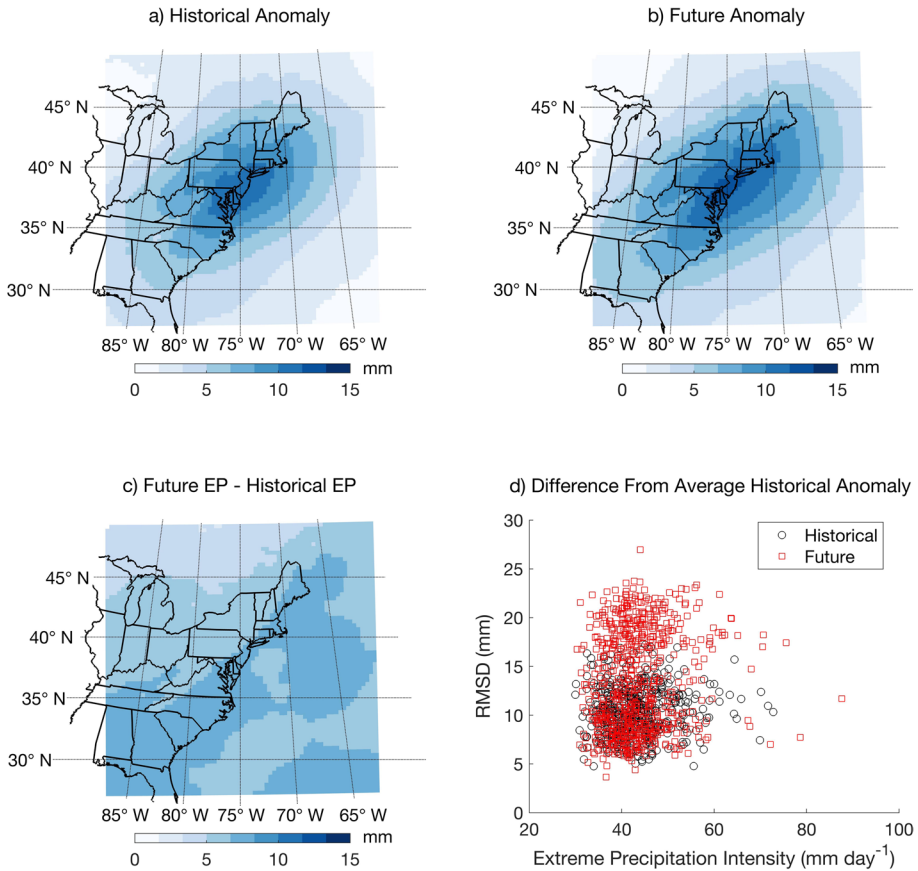
Fig. 9 The CESM-WRF **a** average historical (1986–1995) EP anomaly, **b** average future (2081–2090) EP anomaly, **c** difference between the average future EP day and the average historical EP day, and **d** differences between historical and future EP days and the average historical EP anomaly, for precipitable water

despite not being as large as in the southeastern USA. Figure 9d compares the precipitable water anomaly pattern on each historical and future EP day with the precipitable water anomaly pattern on the average EP day in the historical record. We find that while there are many EP days where the future precipitable water anomaly is markedly larger (higher RMSD in Fig. 9d, net increase in average precipitable water in Fig. 9c), these days are not associated with heavier amounts of EP, but instead generally fall within the historical EP events range of 30 to 60 mm (Fig. 9d).

The historical and future 500 mb wind anomaly plots (Fig. 10a, b) show increased anticyclonic flow centered over far northeastern Maine, resulting in enhanced southerly and southeasterly winds driving moisture into the Northeast from the Atlantic Ocean. These circulation pattern on EP days can draw moisture from south of the Northeast, where there are greater changes in precipitable water (Fig. 9c). However, across the domain differences between historical and future 500 mb winds on EP days reveal a small (< 1 m s^{-1}) weakening in anticyclonic flow centered over Vermont, New Hampshire, and Maine (Fig. 10c). The very small changes in the magnitude of 500 mb winds
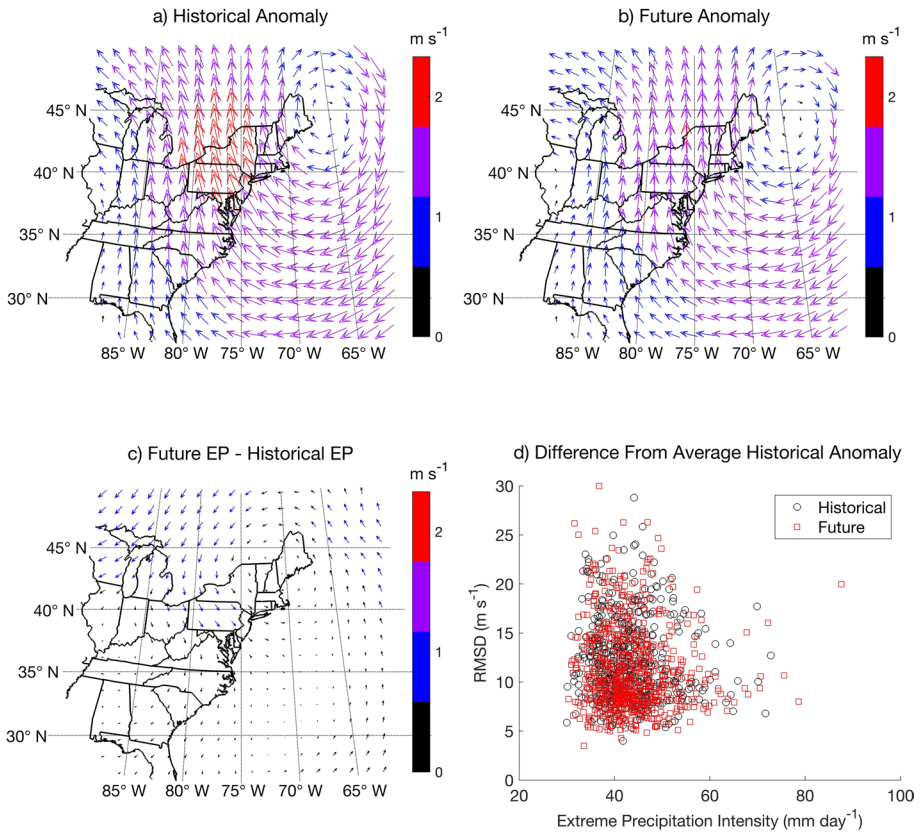
Fig. 10 The CESM-WRF **a** average historical (1986–1995) EP anomaly, **b** average future (2081–2090) EP anomaly, **c** difference between the average future EP day and the average historical EP day, and **d** differences between historical and future EP days and the average historical EP anomaly, for 500 mb winds

over the twenty-first century are apparent in Fig. 10d, which shows the markers for historical and future winds clustered closely together, emphasizing that projected 500 mb winds on future EP days are very similar to the 500 mb winds simulated on historical EP days. We repeated this analysis for 250 mb winds to understand changes at other vertical pressure levels (not shown) and found patterns similar to Fig. 10.

Figures 11 a and b show a strong low-pressure anomaly over the majority of the Northeast, Mid-Atlantic, and Midwestern states in both historical and future sea level pressure anomaly plots. This indicates a concentration of low-pressure systems on EP days and is accompanied by pronounced high-pressure in the upper right corner of the domain (Fig. 11a, b). Unlike the anomaly plots, Fig. 11c reveals that overall sea level pressure on future EP days is projected to be slightly higher than on historical EP days across most of the Northeast. Similar to 500 mb winds, we find that the difference between sea level pressure anomalies on future and historical EP days is small (Fig. 11c, d).
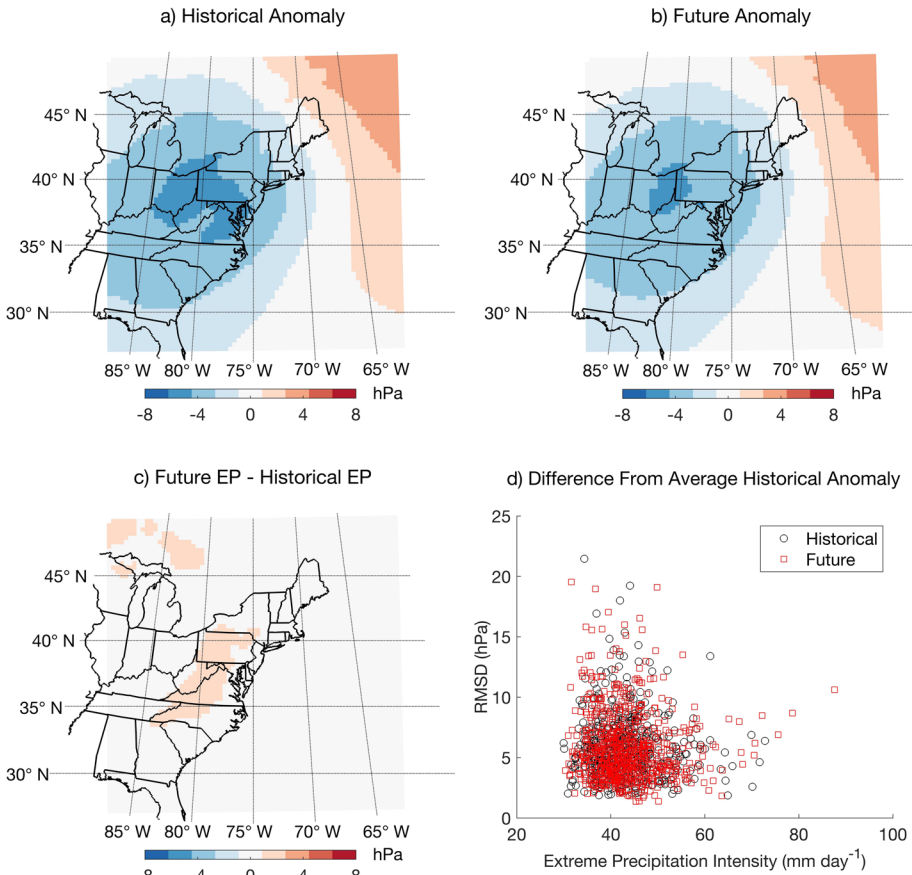
Fig. 11 The CESM-WRF **a** average historical (1986–1995) EP anomaly, **b** average future (2081–2090) EP anomaly, **c** difference between the average future EP day and the average historical EP day, and **d** differences between historical and future EP days and the average historical EP anomaly, for sea level pressure

4 Discussion

4.1 Total and extreme precipitation biases

Compared to Daymet, CESM-WRF and ESM-WRF simulate excess precipitation and wet days for most seasons, generally consistent with previous evaluations of WRF precipitation over the Northeast (Loikith et al. 2018; Huang et al. 2020). Both CESM-WRF and ESM-WRF, despite having different overall annual biases, underestimate TP intensity annually and in each season. While the vast majority of TP biases are less than 300 mm, there are some areas where maximum biases can exceed 300 mm. These maximum biases primarily occur in urban areas, such as Syracuse, Boston, and Pittsburgh, and in regions near water bodies that are not large enough to be masked out (e.g., Lake Champlain and Moosehead Lake).

CESM-WRF and ESM-WRF simulations of EP over1980-2005 have wet biases annually and for all seasons, except for CESM-WRF fall. This is consistent with Huang et al. (2020), who found that WRF tends to overestimate extreme precipitation more than total

precipitation. CESM-WRF simulations of EP have the same general spatial patterns of precipitation bias as TP; however, the magnitudes of the EP biases are larger. These larger EP biases are expected, as previous literature has shown that WRF simulations can reproduce the majority of the precipitation distribution but struggle to accurately simulate the tail (Huang et al. 2020). CESM-WRF and ESM-WRF both simulate excess EP days compared to Daymet annually and throughout each season. The similarity between wet day and EP day frequency biases for CESM-WRF and ESM-WRF is a result of EP being defined as the amount of precipitation falling on the top 1% of wet days recording the most precipitation (Huang et al. 2017). Therefore, the number of EP days each year is directly linked to the number of wet days. We evaluate precipitation biases in this manuscript primarily to provide context for simulated precipitation changes; and while Loikith et al. (2018) and Huang et al. (2020) do assess some relationships between model configuration and bias, additional work that explores the causes of the WRF TP and EP biases (e.g., parameterizations, boundary conditions, domain, resolution) is critical to improving precipitation projections for the Northeast.

4.2 Changes in total and extreme precipitation

The 9.7% increase in annual total precipitation projected by CESM-WRF is consistent with ESM-WRF projections of a 10.8% increase, and with Hayhoe et al. (2007) who projected a 14% increase in annual precipitation by the end of the century under the A1FI emissions scenario. We find that CESM-WRF projects domain-wide increases in TP by the end of the century, with the largest increases occurring west of the coastal Atlantic. These results agree with Lynch et al. (2016), who determined that the most significant increases in Northeast precipitation are projected to occur in the northern and interior regions. Seasonally, CESM-WRF simulates the largest increases (16.4%) in TP during the winter season, which is consistent with ESM-WRF results but half that of Hayhoe et al. (2007), who found a 30% increase in winter TP by the end of the century over New England, New Jersey, New York, and Pennsylvania under a high emissions scenario.

While CESM-WRF and ESM-WRF both project significant changes in winter and spring TP, they disagree on the magnitude and direction of TP change during the warm season. CESM-WRF projects an increase in summer precipitation and mild decrease in TP during the fall, whereas ESM-WRF projects a slight decrease in summer precipitation and an increase in fall TP. Similar studies have also found strong disagreement between models regarding the direction of warm-season precipitation change (Lynch et al. 2016). Out of the 16 NA-CORDEX models, 13 project statistically significant increases in TP by the end of the century, with 14 models predicting increased fall rainfall. Unlike the fall, 9 NA-CORDEX simulations project summer increases, 6 project decreases, and 1 projects no change. Thus, we conclude that fall precipitation is likely to increase by the end of the twenty-first century despite the decrease projected by CESM-WRF, potentially linked to the large fall dry bias in CESM-WRF.

The 51.6% increase in EP simulated by CESM-WRF across the Northeast is consistent with Hayhoe et al. (2018), who projected increases exceeding 40% for the Northeast by 2070–2099 compared to 1986–2015. We find that CESM-WRF projections of total EP increases are likely conservative, with ESM-WRF projecting that annual EP will increase by approximately 104.2%. Our ESM-WRF findings agree with Thibeault and Seth (2014), who found increases of 100.4% in EP by the late twenty-first century (2071–2099) compared to historical values using 23 CMIP5 coupled models. Overall, 11

of 16 NA-CORDEX simulations project total EP increases between 50 and 100% by the end of the century, suggesting that CESM-WRF and ESM-WRF projections may serve as likely lower and upper bounds on Northeast EP changes, respectively.

Unlike the projected increases in TP intensity and minimal changes in wet day frequency, both CESM-WRF and ESM-WRF project significant increases in EP day frequency, with marginal increases in intensity. The simulated increases in frequency agree with historical changes described in Hoerling et al. (2016), who found that 95th percentile wet day precipitation increases over 1979–2013 were primarily driven by increases in event frequency rather than event intensity. However, we note that our choice to use a consistent EP threshold does affect our calculations of frequency and intensity. While on average EP intensity is not changing, there is an increase in EP days with very large precipitation totals, but it is diluted by a much larger increase in EP days with smaller precipitation totals. If we calculate thresholds separately for historical and future time periods, the increase in CESM-WRF EP intensity is 11.9%, a relatively moderate increase because the smaller, more numerous EP events dominate the mean. The significant increase in the number of EP days explains the increase in TP intensity. As the number of EP days increases in the future and the number of wet days remains relatively unchanged, each individual wet day is expected to experience more rainfall. Therefore, the increased frequency of EP events drives the increased intensity of total annual precipitation.

4.3 Atmospheric drivers of projected precipitation changes

We find that precipitable water is projected to increase markedly (+23.8%) on future EP days compared to historical EP days (Fig. 9c), consistent with projected changes in extreme precipitation. Numerous studies have similarly concluded that increased precipitable water is expected to be a key driver of precipitation change (Hoerling et al. 2016; Lynch et al. 2016; Huang et al. 2018) due to the ability of a warmer atmosphere to hold more water vapor as described by the Clausius-Clapeyron (C–C) relationship. This is consistent with Teale and Robinson (2022), who found enhanced integrated water vapor transport over 1900–2010. To contextualize how simulated increases in precipitable water scale with temperature in our simulations, we analyzed projected changes in temperature in the bottom 20 atmospheric layers, which hold the majority of water vapor. We find that average temperature is projected to increase by approximately 3.7 K by the end of the century. Scaling the C–C relationship of a 7% K^{-1} increase in moisture-holding capacity of the atmosphere (Trenberth et al. 2003), our 3.7 K increase in mean temperature corresponds to a 25.9% increase in precipitable water by the end of the century. CESM-WRF projects precipitable water to increase by 23.8% on future EP days (Fig. 9c) and 25.7% on all future days (not shown), highlighting the consistency of precipitable water changes in our simulations with the C–C relationship.

Precipitable water is projected to be markedly higher on many future EP days compared to historical EP days, as indicated by the higher RMSD in Fig. 9d. This drives an increase in regional EP day frequency (517 days in the historical, 701 days in the future), but does not drive an increase in regional EP intensity. However, as noted above, disentangling frequency and intensity contributions to changing EP is complicated by choice of historical and future EP thresholds.

Enhanced anticyclonic flow over the northeast of the domain and increased southerly and southeasterly flow are associated with EP. These results agree with historical and future anomaly plots for precipitable water, as these winds drive moisture into the Northeast

from the Atlantic. However, we find minimal changes in wind speed (under 1 m s^{-1} for the majority of the domain) between our historical and future anomaly plots. Given the disagreement between anomaly plots, the minimal changes in the difference plot, and the closely overlapping clusters in the scatterplot (Fig. 10), our results suggest that 500 mb winds are not an important driver of increased EP in our simulations.

The last potential driver of change we examined was sea level pressure, and both historical and future anomaly plots indicate that EP days are associated with large low-pressure systems over the Midwest, Mid-Atlantic, and most of the states in the Northeast. These anomaly plots are consistent with anomalies in precipitable water and 500 mb winds as anticyclonic activity over northeastern Maine leads to moisture being driven from the Atlantic into the Northeast region, facilitating rainfall. We find, however, that sea level pressure on future EP days is slightly higher (0.5 hPa) than on historical EP days, and inconsistent with the anomalies associated with EP days, suggesting that changes in sea level pressure are not a significant driver of the projected EP change in the Northeast.

4.4 Implications and future work

Total and extreme precipitation increases can have broad societal and ecological implications for the Northeast. Wolfe et al. (2018) revealed that 34% of Northeast crop losses over 2013–2016 were associated with extreme rainfall events. Increased total and extreme precipitation can reduce agricultural productivity through root anoxia, the spread of foliar diseases by fungi species, and by creating wet soil conditions favorable to root pathogens (Garrett et al. 2006; Wolfe et al. 2018). In addition to direct impacts on crops, increasing EP may also lead to enhanced agricultural runoff of pesticides, herbicides, and other harmful chemicals into the environment (Bloomfield et al. 2006). This increase in surface runoff is increasingly problematic as the demand for herbicides is expected to increase as weeds grow faster due to the changing climate (Bloomfield et al. 2006).

Increases in total and extreme precipitation may also increase regional streamflow, affecting aquatic habitats (Field et al. 2007; Jones et al. 2013). Faster streamflow, combined with higher water temperatures, will degrade aquatic ecosystems for some species (Field et al. 2007; Jones et al. 2013). In addition to aquatic ecosystems, increasing streamflow due to more intense precipitation poses risks to Northeast bridges susceptible to bridge scour (Wright et al. 2012). Wright et al. (2012) found that between 2501 and 5000 bridges in New England are vulnerable to climate change, with a similar amount in the Mid-Atlantic states.

Potential future work includes using different thresholds for EP, analyzing more potential atmospheric drivers of precipitation change, and studying factors that may contribute to the societal impacts of EP. An analysis including thresholds in addition to the top 1% or using different top 1% thresholds for historical and future time periods, would allow for a more comprehensive investigation of the projected changes in EP, EP frequency, and EP intensity. Higher EP thresholds would likely require continuous records longer than 30 years to capture enough rare events for a meaningful analysis. In this study, we examined precipitable water, 500 mb winds, and sea level pressure, but numerous other variables, in particular those related to stability and lift, evapotranspiration and other land surface processes, and connections to large-scale atmospheric patterns, would provide a better understanding of the dynamics behind projected precipitation changes. For example, studies have suggested that decadal ocean variability and sea surface temperatures in the Atlantic Ocean may be important drivers of intense precipitation changes (Hoerling et al.

2016; Huang et al. 2018). In addition, previous literature found that extratropical cyclones are responsible for the majority of cool season precipitation, so examining extratropical cyclone development could illuminate drivers of seasonal precipitation (Zhang and Colle 2017). Llopart et al. (2021) assessed projected changes in the atmospheric water budget and precipitation of an ensemble of CORDEX simulations, finding that the atmospheric water budget variables that drive changes in precipitation vary by region and season. Also, Hayhoe et al. (2007) projected increased evapotranspiration in the Northeast under a warming climate. Lastly, analyses of antecedent soil moisture, precipitation phase, and other factors important to flooding could yield valuable insights into the impacts of total and extreme precipitation changes across the Northeast.

5 Conclusions

Compared to Daymet observations, CESM-WRF hindcasts simulate regionally averaged total precipitation well, with a slight dry bias that is statistically insignificant and occurs primarily along the coast and in New England. Fall is the main contributor to the annual dry bias with all other seasons having insignificant wet biases. CESM-WRF overestimates wet days and underestimates TP intensity. CESM-WRF extreme precipitation biases are larger than TP biases, but the seasonal patterns of EP and TP biases are similar. Seasonal EP biases partially cancel, resulting in an insignificant annual EP wet bias. Spatially, CESM-WRF simulations of annual EP have domain-wide wet biases except for slight drying along the coast from Delaware to southern Maine. Like TP, CESM-WRF overestimates the frequency of EP days during each season and underestimates EP intensity, except in the winter.

Future CESM-WRF simulations (2070–2099) ofNortheast annual TP are 9.7% greater than historical simulations (1976–2005),in close agreement with ESM-WRF simulations and most NA-CORDEX simulations. CESM-WRF simulated significant TP increases for spring, summer, and winter, with winter experiencing the most marked change of 16.4%. ESM-WRF projects no statistically significant summer or fall TP changes, and the 16 NA-CORDEX GCM-RCM pairs vary widely in warm season projections of TP. We conclude that winter and spring increases are likely to drive future TP increases, while changes during the summer and fall seasons remain uncertain, consistent with previous literature. We find that CESM-WRF projects the largest TP increases in West Virginia, central New York, the Lake Champlain Basin, and northern Maine. The increases in TP are caused by increasing daily precipitation intensity, as the number of wet days does not significantly change except during the fall in CESM-WRF simulations.

Extreme precipitation is projected by CESM-WRF to increase 51.6% by the end of the century, with dramatic winter (+109.3%) and spring (+88.8%) increases. These findings are consistent with ESM-WRF projections and NA-CORDEX simulations, which suggest that CESM-WRF changes are conservative. EP increases are largest in West Virginia, parts of Pennsylvania, central New York, and northeastern Maine, with smaller increases occurring along the Atlantic coast and south of Lake Ontario. Unlike TP, increases in EP are not a consequence of more intense events; rather, CESM-WRF and ESM-WRF project the number of EP days to increase markedly across each season. CESM-WRF does simulate EP days with unprecedented intensities, but they are averaged out by the large number of additional smaller EP days, leading to unchanged EP intensity. Increases in EP frequency

are consistent with increases in TP intensity, as the number of wet days is relatively unchanged, while the increase in the number of EP days drives up the intensity of daily TP.

We find domain-wide increases in precipitable water, which likely drive enhanced TP and EP by the end of the twenty-first century. More humid conditions in the Northeast facilitate enhanced precipitation over this region with the most substantial increases over the tropical Atlantic Ocean and southern continental USA. Winds at 500 mb on future and historical EP days are relatively similar, suggesting that changes in 500 mb winds are unlikely to be a substantial driver of future EP changes. Like 500 mb winds, changes in sea level pressure between future and historical EP days are small and inconsistent with historical EP day anomalies, and are therefore unlikely to cause more intense EP events.

This analysis importantly provides evidence that recent increases in extreme precipitation will persist into the future, which has critical implications for infrastructure, flood preparedness and response, food production, sediment transport, tourism, and ecosystems. We caveat that we focus exclusively on precipitation with one threshold for extreme precipitation. Expanding this analysis by examining multiple thresholds and other factors important to societal impacts, such as precipitation phase, multi-day precipitation events, and antecedent soil moisture, could yield valuable insight into future impacts of total and extreme precipitation changes across the Northeast.

Declarations

Conflict of interest The authors declare no competing interests.

References

Akinsanola AA, Kooperman GJ, Reed KA, Pendergrass AG, Hannah WM (2020) Projected changes in seasonal precipitation extremes over the United States in CMIP6 simulations. Environ Res Lett 15(10):104078

Barlow M, Gutowski WJ, Gyakum JR, Katz RW, Lim Y-K, Schumacher RS, Wehner MF, Agel L, Bosilovich M, Collow A, Gershunov A, Grotjahn R, Leung R, Milrad S, Min S-K (2019) North American extreme precipitation events and related large-scale meteorological patterns: A review of statistical methods, dynamics, modeling, and trends. Clim Dyn 53(11):6835–6875. https://doi.org/10.1007/s00382-019-04958-z

Bloomfield JP, Williams RJ, Gooddy DC, Cape JN, Guha P (2006) Impacts of climate change on the fate and behaviour of pesticides in surface and groundwater—A UK perspective. Sci Total Environ 369(1):163–177. https://doi.org/10.1016/j.scitotenv.2006.05.019

Bruyère CL, Rasmussen R, Gutmann E, Done J, Tye M, Jaye A, Prein A, Mooney P, Ge M, Fredrick S (2017) Impact of climate change on Gulf of Mexico hurricanes. *NCAR Tech Note. NCAR/TN535*.

Dupigny-Giroux L-AL, Mecray EL, Lemcke-Stampone MD, Hodgkins GA, Lentz EE, Mills KE, Lane ED, Miller R, Hollinger DY, Solecki WD (2018) Northeast. US Global Change Research Program.

Easterling DR, Kunkel KE, Arnold JR, Knutson T, LeGrande AN, Leung LR, Vose RS, Waliser DE, Wehner MF (2017) Precipitation changes in the United States. Climate Science Special Report: Fourth National Climate Assessment. D. J. Wuebbles et al., Eds.

Field CB, Mortsch LD, Brklacich M, Forbes DL, Kovacs P, Patz JA, Running SW, Scott MJ, Andrey J, Cayan D (2007). North America. Climate Change 2007: Impacts, Adaptation and Vulnerability.

Frei A, Kunkel KE, Matonse A (2015) The Seasonal Nature of Extreme Hydrological Events in the Northeastern United States. J Hydrometeorol 16(5):2065–2085. https://doi.org/10.1175/JHM-D-14-0237.1

Garrett KA, Dendy SP, Frank EE, Rouse MN, Travers SE (2006) Climate change effects on plant disease: Genomes to ecosystems. Annu Rev Phytopathol 44:489–509

Guilbert J, Beckage B, Winter JM, Horton RM, Perkins T, Bomblies A (2014) Impacts of Projected Climate Change over the Lake Champlain Basin in Vermont. J Appl Meteorol Climatol 53(8):1861–1875. https://doi.org/10.1175/JAMC-D-13-0338.1

Gutowski WJ, Ullrich PA, Hall A, Leung LR, O'Brien TA, Patricola CM, Arritt RW, Bukovsky MS, Calvin KV, Feng Z, Jones AD, Kooperman GJ, Monier E, Pritchard MS, Pryor SC, Qian Y, Rhoades AM, Roberts AF, Sakaguchi K, Zarzycki C (2020) The Ongoing Need for High-Resolution Regional Climate Models: Process Understanding and Stakeholder Information. Bull Am Meteorol Soc 101(5):E664–E683. https://doi.org/10.1175/BAMS-D-19-0113.1

Han J, Pan H-L (2011) Revision of Convection and Vertical Diffusion Schemes in the NCEP Global Forecast System. Weather Forecast 26(4):520–533. https://doi.org/10.1175/WAF-D-10-05038.1

Hayhoe K, Wake CP, Huntington TG, Luo L, Schwartz MD, Sheffield J, Wood E, Anderson B, Bradbury J, DeGaetano A, Troy TJ, Wolfe D (2007) Past and future changes in climate and hydrological indicators in the US Northeast. Clim Dyn 28(4):381–407. https://doi.org/10.1007/s00382-006-0187-8

Hayhoe K, Wuebbles DJ, Easterling DR, Fahey DW, Doherty S, Kossin JP, Sweet WV, Vose RS, Wehner MF (2018) Our changing climate. Impacts, risks, and adaptation in the united states: The fourth national climate assessment, volume II.

Hoerling M, Eischeid J, Perlwitz J, Quan X-W, Wolter K, Cheng L (2016) Characterizing Recent Trends in U.S. Heavy Precipitation. J Clim 29(7):2313–2332. https://doi.org/10.1175/JCLI-D-15-0441.1

Hong S-Y, Lim J-OJ (2006) The WRF single-moment 6-class microphysics scheme (WSM6). Asia-Pac J Atmos Sci 42(2):129–151

Huang H, Winter JM, Osterberg EC, Horton RM, Beckage B (2017) Total and Extreme Precipitation Changes over the Northeastern United States. J Hydrometeorol 18(6):1783–1798. https://doi.org/10.1175/JHM-D-16-0195.1

Huang H, Winter JM, Osterberg EC (2018) Mechanisms of Abrupt Extreme Precipitation Change Over the Northeastern United States. J Geophys Res Atmos 123(14):7179–7192. https://doi.org/10.1029/2017JD028136

Huang H, Winter JM, Osterberg EC, Hanrahan J, Bruyère CL, Clemins P, Beckage B (2020) Simulating precipitation and temperature in the Lake Champlain basin using a regional climate model: Limitations and uncertainties. Clim Dyn 54(1):69–84. https://doi.org/10.1007/s00382-019-04987-8

Huang H, Patricola CM, Winter JM, Osterberg EC, Mankin JS (2021) Rise in Northeast US extreme precipitation caused by Atlantic variability and climate change. Weather Clim Extremes 33:100351. https://doi.org/10.1016/j.wace.2021.100351

Iacono MJ, Delamere JS, Mlawer EJ, Shephard MW, Clough SA, Collins WD (2008) Radiative forcing by long-lived greenhouse gases: Calculations with the AER radiative transfer models. J Geophys Res Atmos 113(D13). https://doi.org/10.1029/2008JD009944

Janjić ZI (1994) The Step-Mountain Eta Coordinate Model: Further Developments of the Convection, Viscous Sublayer, and Turbulence Closure Schemes. Mon Weather Rev 122(5):927–945. https://doi.org/10.1175/1520-0493(1994)122%3c0927:TSMECM%3e2.0.CO;2

Jones R, Travers C, Rodgers C, Lazar B, English E, Lipton J, Vogel J, Strzepek K, Martinich J (2013) Climate change impacts on freshwater recreational fishing in the United States. Mitig Adapt Strat Glob Change 18(6):731–758. https://doi.org/10.1007/s11027-012-9385-3

Kunkel KE, Karl TR, Brooks H, Kossin J, Lawrimore JH, Arndt D, Bosart L, Changnon D, Cutter SL, Doesken N, Emanuel K, Groisman PY, Katz RW, Knutson T, O'Brien J, Paciorek CJ, Peterson TC,

Redmond K, Robinson D, Wuebbles D (2013) Monitoring and Understanding Trends in Extreme Storms: State of Knowledge. Bull Am Meteorol Soc 94(4):499–514. https://doi.org/10.1175/BAMS-D-11-00262.1

Llopart M, Domingues LM, Torma C, Giorgi F, da Rocha RP, Ambrizzi T, Reboita MS, Alves LM, Coppola E, da Silva ML, de Souza DO (2021) Assessing changes in the atmospheric water budget as drivers for precipitation change over two CORDEX-CORE domains. Clim Dyn 57(5):1615–1628. https://doi.org/10.1007/s00382-020-05539-1

Loikith PC, Waliser DE, Kim J, Ferraro R (2018) Evaluation of cool season precipitation event characteristics over the Northeast US in a suite of downscaled climate model hindcasts. Clim Dyn 50(9):3711–3727. https://doi.org/10.1007/s00382-017-3837-0

Lynch C, Seth A, Thibeault J (2016) Recent and Projected Annual Cycles of Temperature and Precipitation in the Northeast United States from CMIP5. J Clim 29(1):347–365. https://doi.org/10.1175/JCLI-D-14-00781.1

Maloney ED, Camargo SJ, Chang E, Colle B, Fu R, Geil KL, Hu Q, Jiang X, Johnson N, Karnauskas KB, Kinter J, Kirtman B, Kumar S, Langenbrunner B, Lombardo K, Long LN, Mariotti A, Meyerson JE, Mo KC, Zhao M (2014) North American Climate in CMIP5 Experiments: Part III: Assessment of Twenty-First-Century Projections. J Clim 27(6):2230–2270. https://doi.org/10.1175/JCLI-D-13-00273.1

McGinnis S (2021) NA-CORDEX Bias Correction Error. Available online at: https://na-cordex.org/bias-correction-error.html

Mearns LO, McGinnis S, Korytina D, Arritt R, Biner S, Bukovsky M, Chang HI, Christensen O, Herzmann D, Jiao Y (2017) The NA-CORDEX dataset, version 1.0. NCAR climate data gateway, boulder CO.

Mesinger F (1993) Forecasting upper tropospheric turbulence within the framework of the Mellor-Yamada 2.5 closure. Res Activ Atmos Oceanic Mod.

Moss RH, Edmonds JA, Hibbard KA, Manning MR, Rose SK, van Vuuren DP, Carter TR, Emori S, Kainuma M, Kram T, Meehl GA, Mitchell JFB, Nakicenovic N, Riahi K, Smith SJ, Stouffer RJ, Thomson AM, Weyant JP, Wilbanks TJ (2010) The next generation of scenarios for climate change research and assessment. Nature 463(7282):747–756. https://doi.org/10.1038/nature08823

Rasmussen B, Lamoureux K, Simmons E, Miller R (2018) *U.S. Forest Service Transportation Resiliency Guidebook: Addressing Climate Change Impacts on U.S. Forest Service Transportation Assets* (dot:38737). *DOT-VNTSC-USDA-19–01*. https://rosap.ntl.bts.gov/view/dot/38737

New Hampshire Coastal Risk and Hazards Commission (2016) Preparing New Hampshire for Projected Storm Surge, Sea-Level Rise, and Extreme Precipitation: Final Report and Recommendations. https://www.nhcrhc.org/wp-content/uploads/2016-CRHC-final-report.pdf

Skamarock WC, Klemp JB, Dudhia J et al (2008) A description of the advanced research WRF version 3. NCAR Technical Note NCAR/TN-475 + STR. https://doi.org/10.5065/D68S4MVH

Teale N, Robinson DA (2022) Long-term variability in atmospheric moisture transport and relationship with heavy precipitation in the eastern USA. Clim Change 175(1):1. https://doi.org/10.1007/s10584-022-03455-3

Thibeault JM, Seth A (2014) Changing climate extremes in the Northeast United States: Observations and projections from CMIP5. Clim Change 127(2):273–287. https://doi.org/10.1007/s10584-014-1257-2

Thornton PE, Running SW, White MA (1997) Generating surfaces of daily meteorological variables over large regions of complex terrain. Aggregate Description Land-Atmos Interact 190(3):214–251. https://doi.org/10.1016/S0022-1694(96)03128-9

Thornton PE, Thornton MM, Mayer BW, Wei Y, Devarakonda R, Vose RS, Cook RB (2016) Daymet: Daily Surface Weather Data on a 1-km Grid for North America, Version 3. https://doi.org/10.3334/ORNLDAAC/1328

Trenberth KE, Dai A, Rasmussen RM, Parsons DB (2003) The Changing Character of Precipitation. Bull Am Meteor Soc 84(9):1205–1218. https://doi.org/10.1175/BAMS-84-9-1205

Walsh J, Wuebbles D, Hayhoe K, Kossin J, Kunkel K, Stephens G, Thorne P, Vose R, Wehner M (2014) Our Changing Climate. Climate Change Impacts in the United States: The Third National Climate Assessment: 19–67. US Global Change Research Program.

Wolfe DW, DeGaetano AT, Peck GM, Carey M, Ziska LH, Lea-Cox J, Kemanian AR, Hoffmann MP, Hollinger DY (2018) Unique challenges and opportunities for northeastern US crop production in a changing climate. Clim Change 146(1):231–245. https://doi.org/10.1007/s10584-017-2109-7

Wright L, Chinowsky P, Strzepek K, Jones R, Streeter R, Smith JB, Mayotte J-M, Powell A, Jantarasami L, Perkins W (2012) Estimated effects of climate change on flood vulnerability of U.S. bridges. Mitig Adapt Strateg Glob Chang 17(8):939–955. https://doi.org/10.1007/s11027-011-9354-2

Zhang Z, Colle BA (2017) Changes in Extratropical Cyclone Precipitation and Associated Processes dur-
ing the Twenty-First Century over Eastern North America and the Western Atlantic Using a Cyclone-
Relative Approach. J Clim 30(21):8633–8656. https://doi.org/10.1175/JCLI-D-16-0906.1

Zhang X, Hogg WD, Mekis É (2001) Spatial and Temporal Characteristics of Heavy Precipitation Events
over Canada. J Clim 14(9):1923–1936. https://doi.org/10.1175/1520-0442(2001)014%3c1923:SAT-
COH%3e2.0.CO;2

Zhang X, Alexander L, Hegerl GC, Jones P, Tank AK, Peterson TC, Trewin B, Zwiers FW (2011) Indices
for monitoring changes in extremes based on daily temperature and precipitation data. Wires Clim
Change 2(6):851–870. https://doi.org/10.1002/wcc.147